Supplementary Information for

Fully Conjugated Tetraborylethylene: Selenium Mediated C–C Double Bond Formation from Diborylcarbenoid

Yuki Shibutani, Shuhei Kusumoto*, and Kyoko Nozaki

kusumoto@tmu.ac.jp

Department of Chemistry, Faculty of Science, Tokyo Metropolitan University, 1-1
Minamiosawa, Hachioji, Tokyo 129-0397, Japan

I. Experimental Section

V. Method and Discussion for Theoretical Calculation

I. Experimental section

I-I. General, Instrumentation and Materials

General

All reactions were carried out using a standard glovebox or Schlenk techniques under nitrogen or argon gas purified by passing through Nikka Seiko dry column DC-L4 (NIKKA SEIKO Co., Ltd.).

Instrumentation

Nuclear magnetic resonance (NMR) spectra were recorded on BRUKER Ascend500 (^{1}H: 500 MHz, ^{13}C: 126 MHz, ^{11}B: 160 MHz, ^{77}Se: 95.4 MHz with digital resolution of 0.305, 0.908, 0.98, 6.73 Hz, respectively) or JEOL ECS400 (^{1}H: 400 MHz, ^{11}B 128 MHz with digital resolution of 0.11, 19.69 Hz) at ambient temperature unless otherwise noted. Chemical shifts are reported in ppm relative to the residual protiated solvent for ^{1}H (benzene-d_6 (C_6D_6) 7.16 ppm, toluene-d_8 2.08 ppm), the deuterated solvent for ^{13}C (C_6D_6 128.06 ppm, toluene-d_8 20.43 ppm), external $(C_2H_5)_2O{\cdot}BF_3$ standard for ^{11}B nuclei, and external $(CH_3)_2Se$ for ^{77}Se nuclei. Mass spectra (MS) were taken with an electron spray ionization time-of-flight (ESI-TOF) method on a JEOL JMS-T100LP AccuTOF LC-plus mass spectrometer. Infrared (IR) spectra were recorded on a JASCO FTIR-6600 equipped with an attenuated total reflection (ATR) system or Agilent Cary 630 FTIR. X-ray crystallographic analyses were performed on a Rigaku Varimax dual with hybrid photon counting detector. UV-Vis spectra were recorded on a SHIMADZU UV-3150 spectrophotometer. Cyclic voltammetry (CV) measurement was conducted on an ALS Model 619Ep Electrochemical Analyzer. Photoluminescence spectra were recorded on JASCO FP8500 spectrofluorometer.

Materials

Anhydrous hexane and tetrahydrofuran (THF) was purchased from Kanto Chemical Co., Inc. (Kanto) and purified by the method of Pangborn et al.[1] The following solvents and reagents were purchased and used as received: benzene, dehydrated -super- (FUJIFILM Wako Pure Chemical Co., Ltd. (Wako)), selenium (Kanto), sulfur (Kanto), tetrabutylammonium hexafluorophosphate (TCI), tris(2-phenylpyridinato)iridium(III) (*fac*-Ir(ppy)$_3$, TCI). C_6D_6 (Aldrich), toluene-d_8 (Aldrich), and hexamethyldisiloxane (TCI) were dehydrated with preactivated molecular sieves 3A (purchased from Nakarai Tesque Co., Ltd.). Compound **1** was prepared according to the literature procedures.[2]

I-II. Preparation of Tetraborylethylene 2

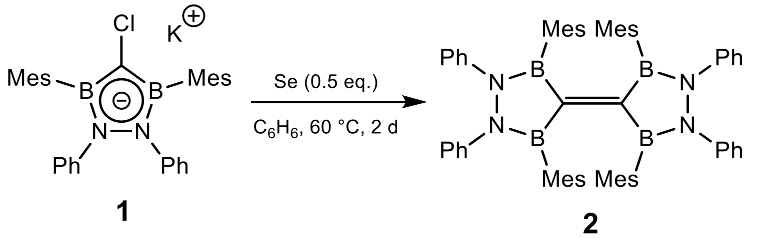

Scheme S1. Synthesis of **2**.

Compound **2**

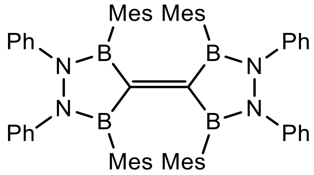

To a suspension of **1** (16.9 mg, 0.032 mmol) in benzene (10 mL), selenium powder (1.1 mg, 0.014 mmol) was added at ambient temperature. Soon after mixing, the color of the reaction solution got purple. The reaction mixture was heated to 60 °C with stirring. During the reaction, the color of the reaction solution gradually changed from purple to red. After 2 days reaction, insoluble stuff was filtered off with a PTFE syringe filter and the solvent was removed under reduced pressure to afford red solid of compound **2** (13.9 mg, 96%). Recrystallization from a hexane solution by slow evaporation gave red crystals of **2** suitable for scXRD analysis.

^{1}H NMR (C_6D_6, 500 MHz) δ: 6.93 (d, *J* = 7.5 Hz, 4H, Ar–*H* (Ph, *o*-)), 6.68 (t, *J* = 7.5 Hz, 4H, Ar–*H* (Ph, *m*-)), 6.47–6.44 (two signals are overlapping; s, 4H, Ar–*H* (Mes) and t, *J* = 7.5 Hz, 2H, Ar–*H* (Ph, *p*-)), 2.19–2.17 (two signals are overlapping; s, 6H and s, 12H (Ar–C*H*)); ^{13}C NMR (C_6D_6, 126 MHz, one signal is missing due to overlapping with the solvent signal.) δ: 195.6 (broadened due to the quadrupole coupling with boron nuclei), 143.2, 139.9, 137.3 (br.), 136.3, 127.4, 124.8, 124.3, 23.8, 21.5; ^{11}B{^{1}H} NMR (C_6D_6, 160 MHz) δ: 31.4; HRMS (ESI) *m/z* calced. for $C_{62}H_{64}B_4KN_4^+$ [M+K$^+$] 947.5135, found 947.5102; IR (neat) cm^{-1} 2918, 2849, 1683, 1597, 1491, 1431, 1337, 1261, 1235, 1186, 1142, 1075, 1038, 1011.

I-III. Generation of Compound 3_{Se} and Decomposition into Compound 2

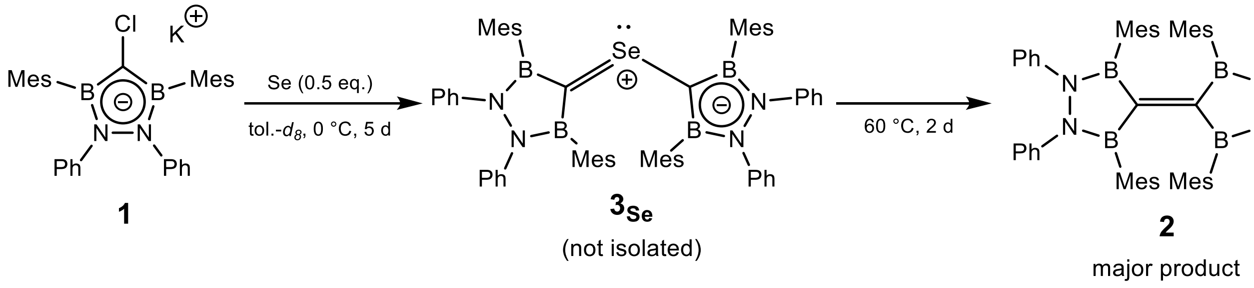

Scheme S2. Formation of compound **3**$_{Se}$ and decomposition into compound **2**.

Compound $\mathbf{3_{Se}}$

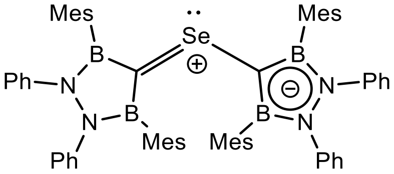

In a J-Young NMR tube, 15.4 mg (0.029 mmol) of compound **1** and selenium powder (1.1 mg, 0.014 mmol) were suspended in toluene-*d₈* (500 µL) at –35 °C. The reaction mixture was settled at 0 °C for 5 days. Soon after mixing of compound **1** and selenium, the color of the reaction solution got dark purple. After 5 days, the reaction solution was analyzed by ^{1}H, ^{13}C, ^{11}B{^{1}H} and ^{77}Se NMR to confirm the generation of $\mathbf{3_{Se}}$ (see Figures S4–S7).

By heating the resultant purple solution containing compound $\mathbf{3_{Se}}$ as the major product at 60 °C for 2 days, compound **2** was observed as a major product (50% NMR yield based on Ar-C*H* integration) with unidentified impurities (see Figure S8 for ^{1}H NMR spectrum). Even at room temperature, conversion of compound $\mathbf{3_{Se}}$ into compound **2** was observed to make it difficult to fully characterize $\mathbf{3_{Se}}$ by spectroscopic analyses. Purple solid left after evaporation of reaction solution was dissolved in hexane and concentrated slowly at room temperature to afford purple-colored, block-shaped single crystals of compound $\mathbf{3_{Se}}$ suitable for scXRD analysis.

^{77}Se NMR (Toluene-*d₈*, 95.4 MHz) δ: 1421; HRMS (ESI) *m/z* calced. for $C_{64}H_{67}B_4N_5Se^+$ [M$^+$ + CH$_3$CN] 1029.4928, found 1029.4889.

I-IV. Synthesis of Compound $\mathbf{3_S}$

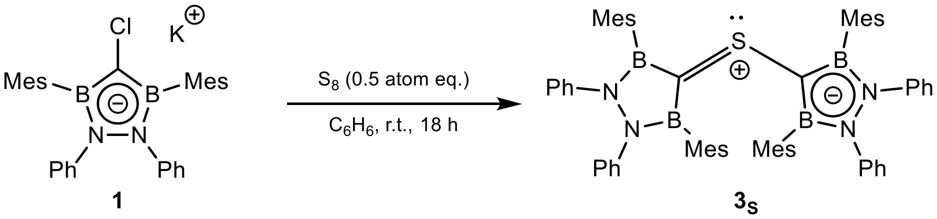

Scheme S3. Synthesis of compound $\mathbf{3_S}$.

Compound $\mathbf{3_S}$

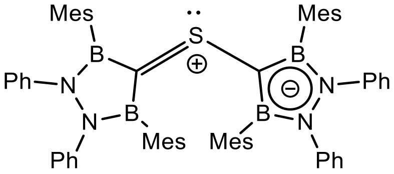

Compound **1** (41.4 mg, 78.3 µmol) was suspended in benzene (3 mL), then 2.5 µL of a stock solution of S$_8$ in benzene (1 µg/µL) was added at room temperature. Soon after the addition of S$_8$, the color of the reaction mixture got dark orange. After stirred at room temperature for 18 hours, insoluble stuff was filtered off with PTFE membrane filter, then all the volatiles were removed under reduced pressure. The residue was extracted with HMDSO (10 mL) and settled at –35 °C for 1 week for recrystallization to afford red tiny crystals of compound $\mathbf{3_S}$ (2.4 mg, 7% yield).

^{1}H NMR (C$_6$D$_6$, 400 MHz) δ: 6.99–6.50 (28H, Ar–*H*), 2.49–2.04 (36H, Ar–C*H*); ^{13}C NMR (C$_6$D$_6$, 126 MHz) δ: 155.0, 142.8, 140.0, 139.5, 137.3, 136.8, 134.4, 129.5, 124.3, 123.8, 122.8, 112.6, 22.7, 22.3, 21.6, 21.4, 21.2; ^{11}B{^{1}H} NMR (C$_6$D$_6$, 128 MHz) δ: 37.8; HRMS (ESI) *m/z* calced. for $C_{62}H_{64}B_4KN_4S^+$ [M+K$^+$] 979.4855, found 979.4847; IR (neat) cm^{-1} 2907, 1595, 1491, 1360, 1301, 1189.

I-V. Reaction of Compound 1 with Excess Amount of Selenium

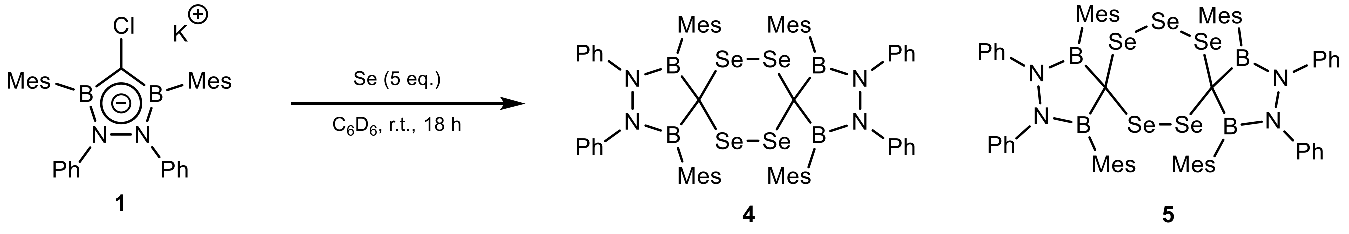

(comfirmed by HRMS and scXRD)

Scheme S4. Reaction of compound **1** with excess amount of selenium.

To a suspension of compound **1** (14.3 mg, 27 μmol) in C_6D_6 (0.5 mL), selenium powder (11.7 mg, 148 μmol) was added at ambient temperature. After 18 hours, the reaction mixture was analyzed by ^{1}H and ^{77}Se NMR (Figure S13 and S14). A trace amount of yellow crystal was obtained from hexane and the component was characterized to be a 15 : 85 mixture of compounds **4** and **5**. Although compounds **4** and **5** were confirmed by scXRD and HRMS, due to the low yield, could not be isolated, and any spectroscopic data could not be obtained.

HRMS (ESI) *m/z* calced for $C_{62}H_{64}B_4NaN_4Se_4^+$ [M+Na$^+$] 1251.2056, found 1251.2087, *m/z* calced for $C_{62}H_{64}B_4KN_4Se_5^+$ [M+K$^+$] 1347.0961, found 1347.0997.

II. NMR Spectra

Compound **2**

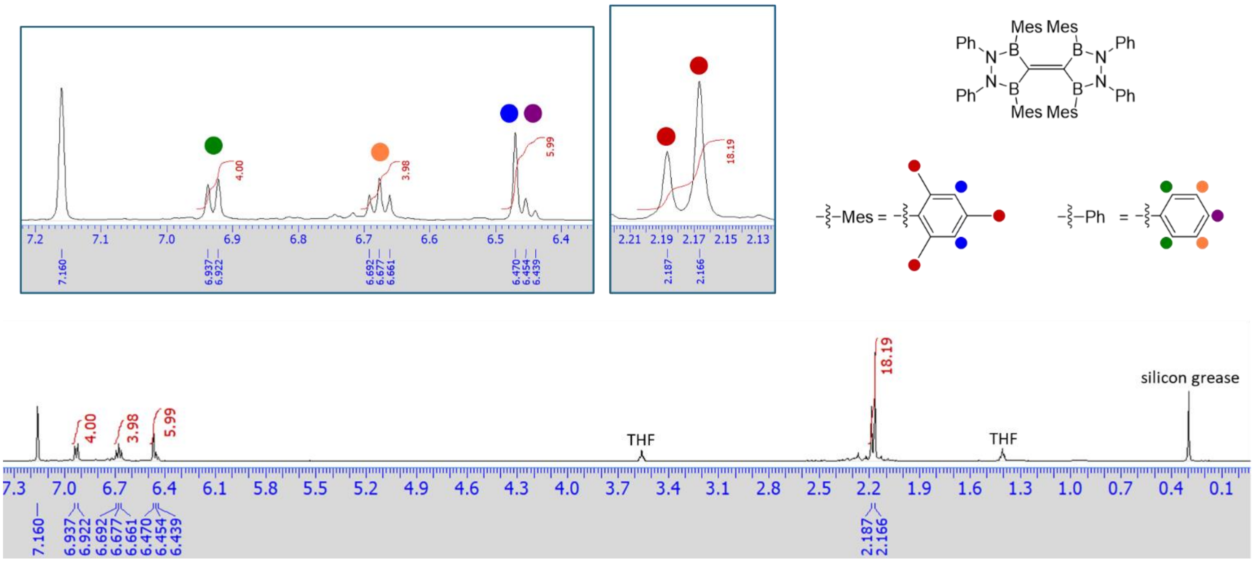

Figure S1. ^{1}H NMR spectrum of compound **2** (C_6D_6, 500 MHz).

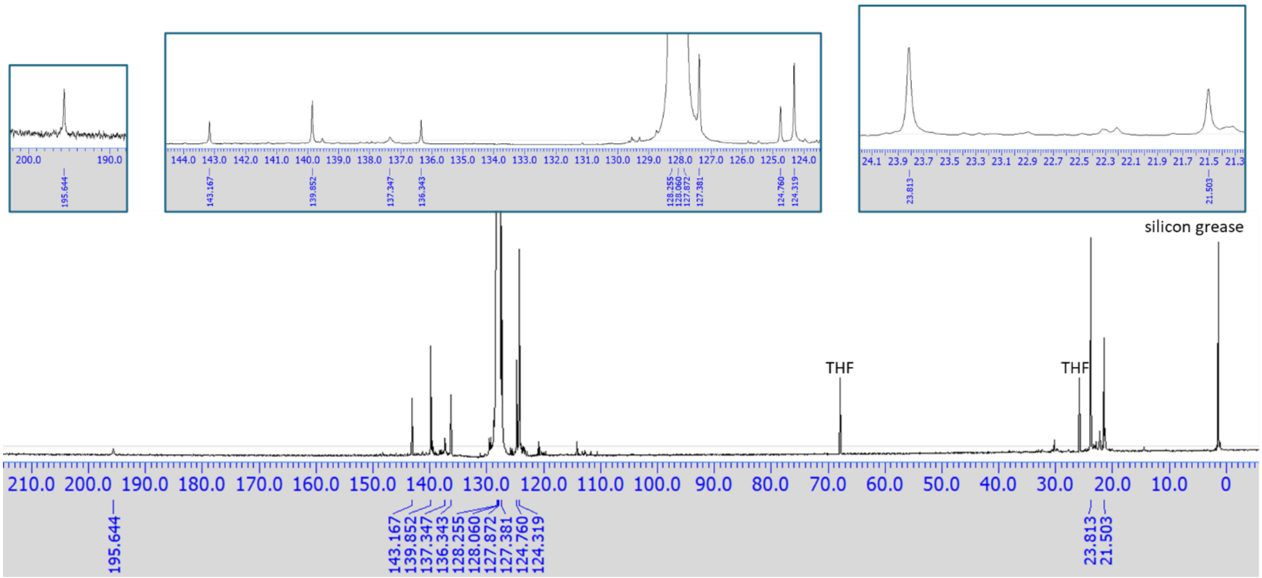

Figure S2. ^{13}C NMR spectrum of compound **2** (C_6D_6, 126 MHz).

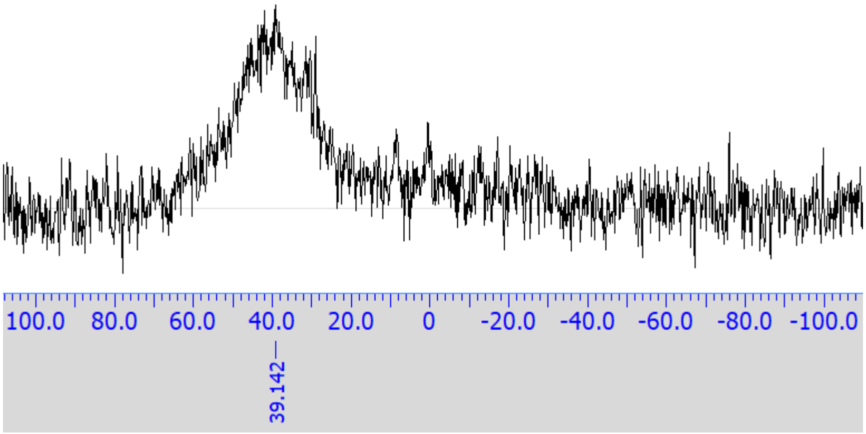

Figure S3. ^{11}B{^{1}H} NMR spectrum of compound **2** (C_6D_6, 128 MHz).

Compound **3**$_{\mathbf{Se}}$

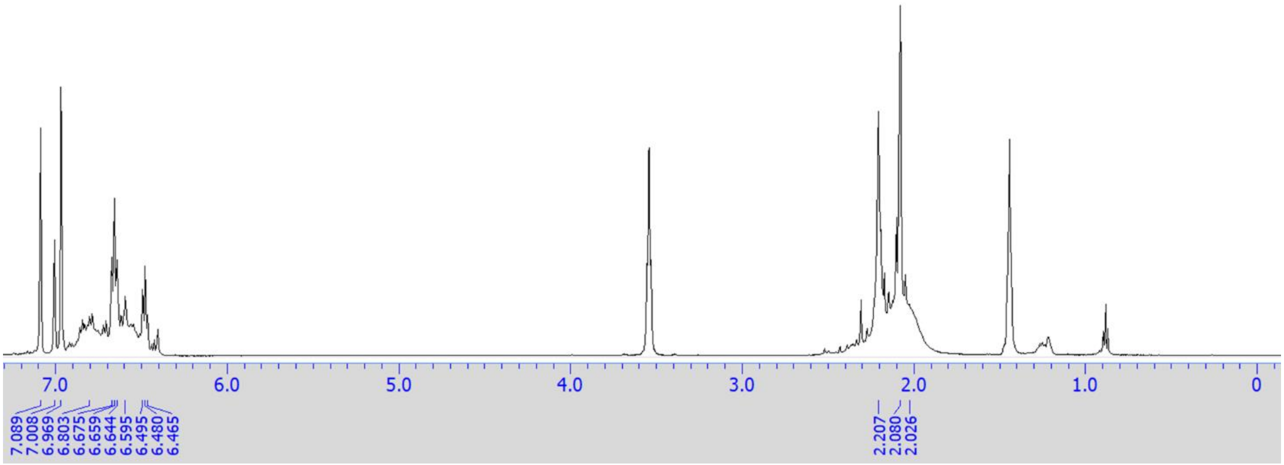

Figure S4. ^{1}H NMR spectrum after reaction of compound **1** with selenium at 0 °C (Toluene-d_8, 500 MHz).

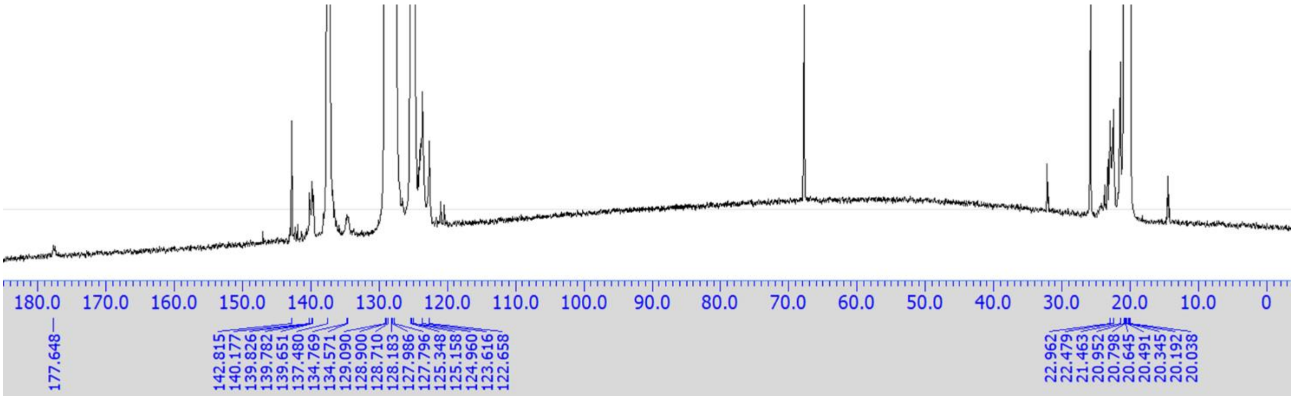

Figure S5. ^{13}C NMR spectrum after reaction of compound **1** with selenium at 0 °C (Toluene-d_8, 126 MHz).

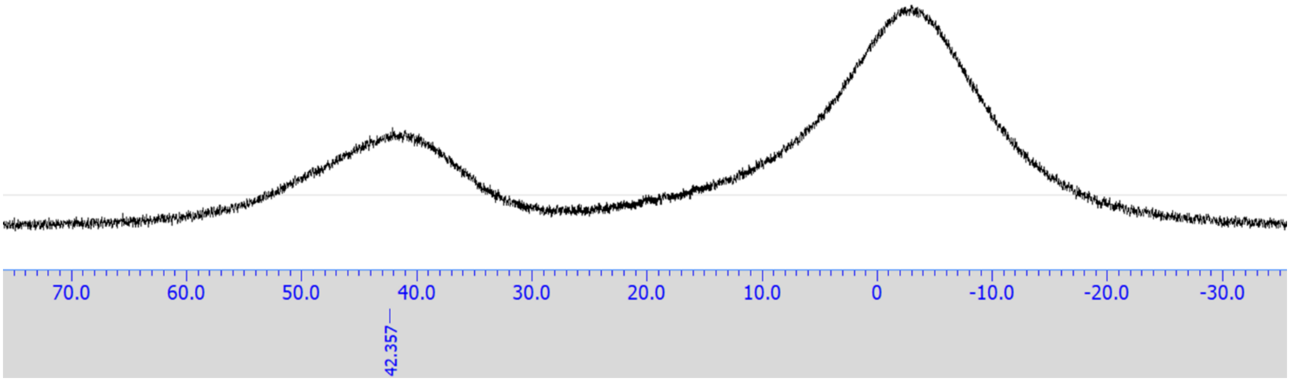

Figure S6. ^{11}B{^{1}H} NMR spectrum after reaction of compound **1** with selenium at 0 °C (Toluene-d_8, 160 MHz).

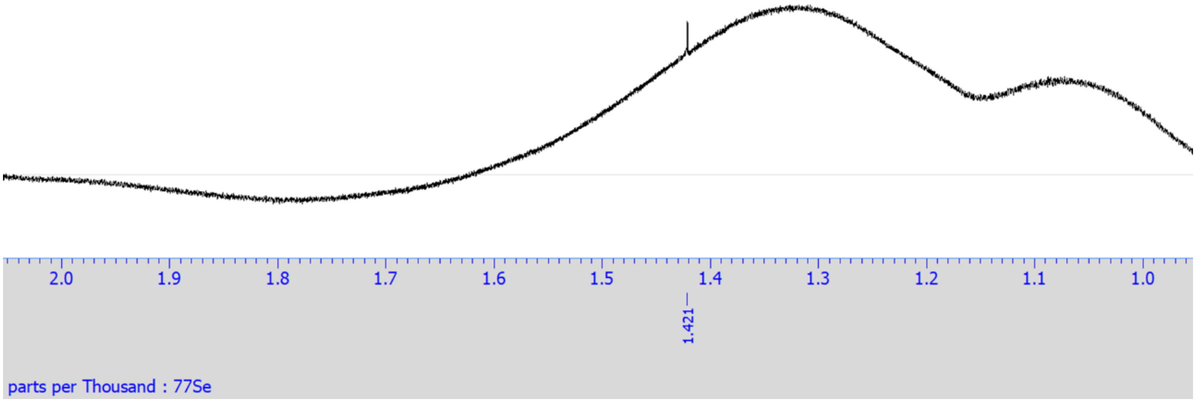

Figure S7. ^{77}Se NMR spectrum after reaction of compound **1** with selenium at 0 °C (Toluene-d_8, 95.4 MHz).

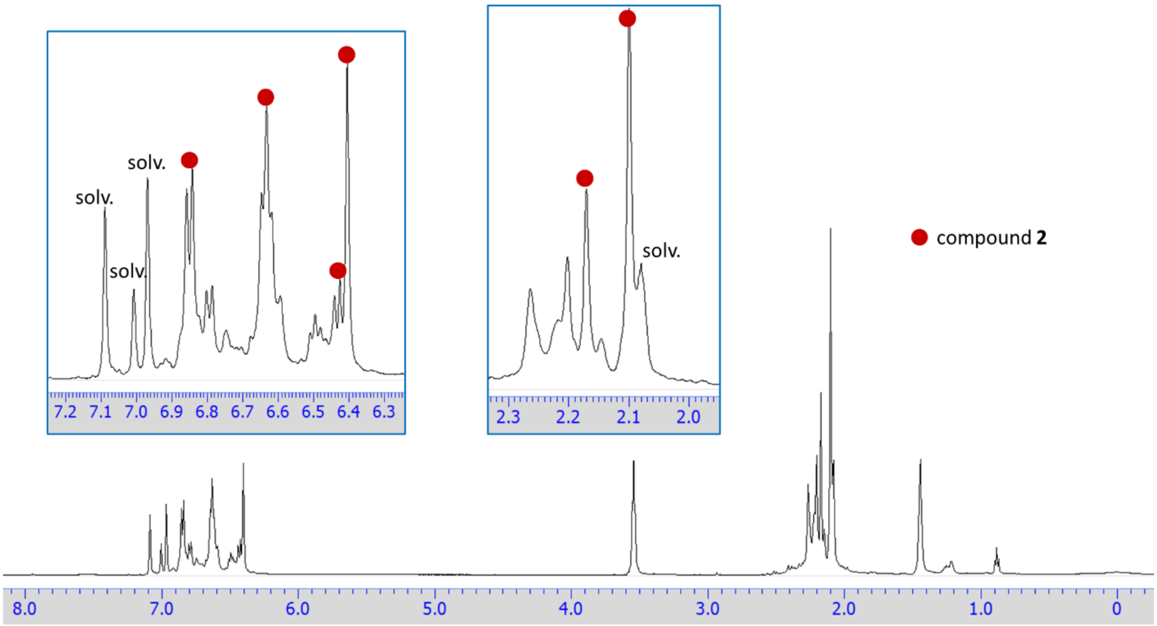

Figure S8. ^{1}H NMR spectrum after heating of compound $\mathbf{3_{Se}}$ at 60 °C (Toluene-d_8, 500 MHz).

Compound $\mathbf{3_{S}}$

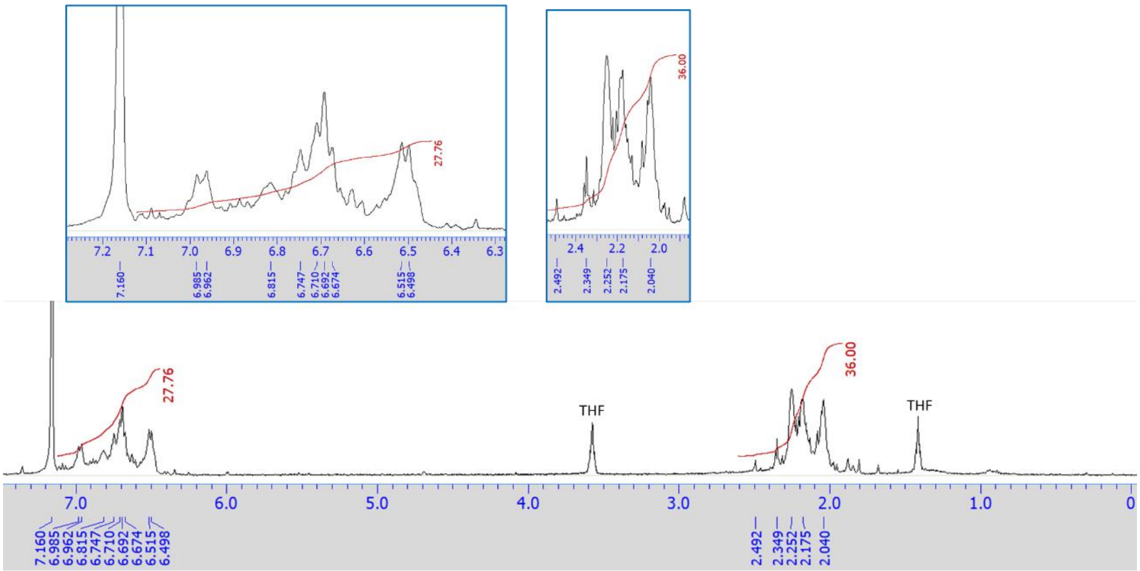

Figure S9. ^{1}H NMR spectrum of compound $\mathbf{3_{S}}$ (C_6D_6, 400 MHz).

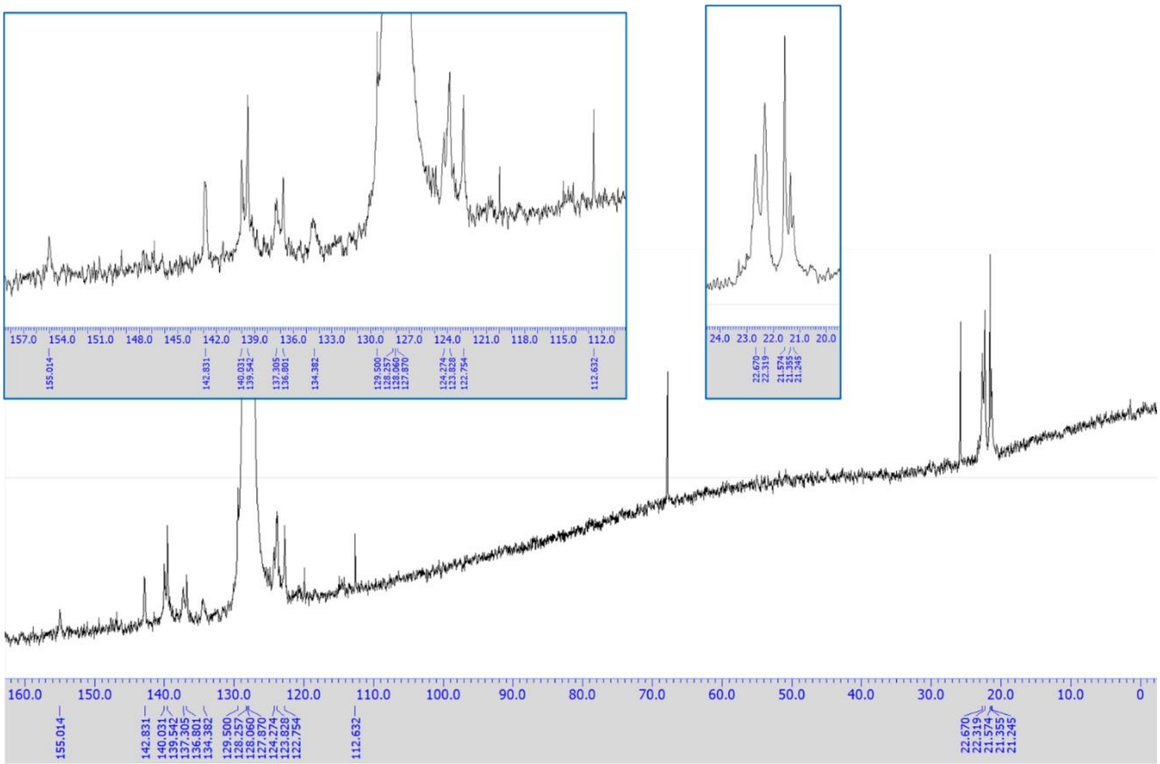

Figure S10. ^{13}C NMR spectrum of compound **3s** (C_6D_6, 126 MHz).

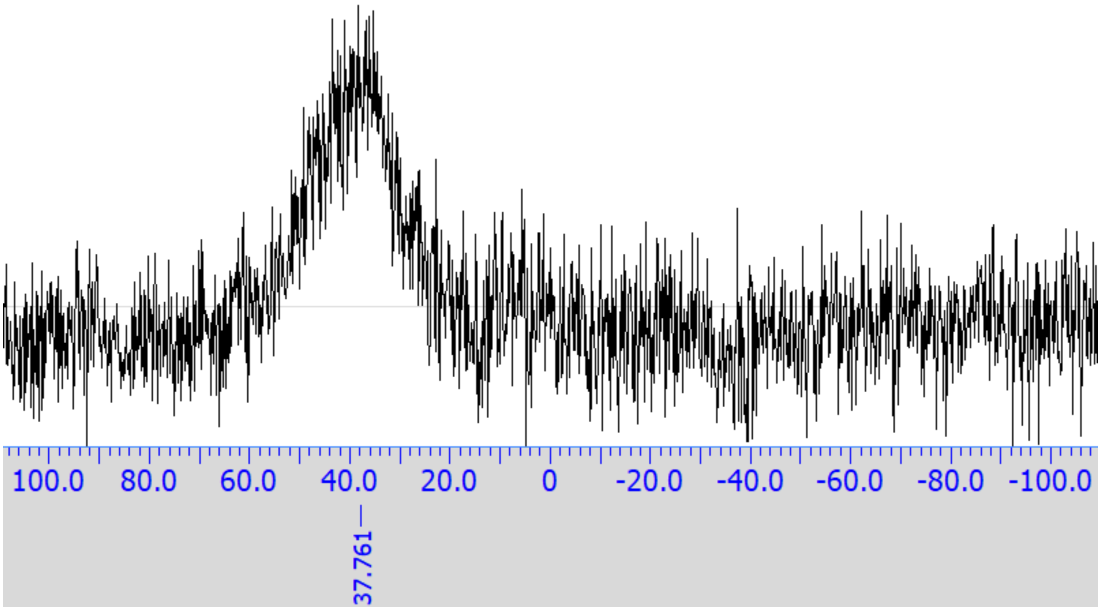

Figure S11. ^{11}B{^{1}H} NMR spectrum of compound **3s** (C_6D_6, 128 MHz).

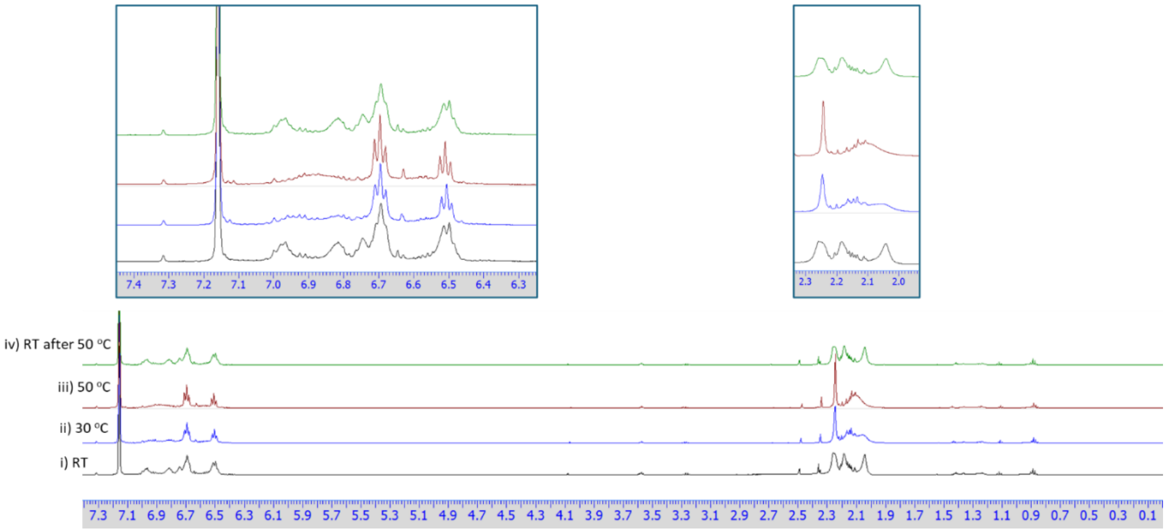

Figure S12. VT-^{1}H NMR spectra of compound **3**$_\mathbf{S}$ from 298 K to 348 K (C_6D_6, 500 MHz).

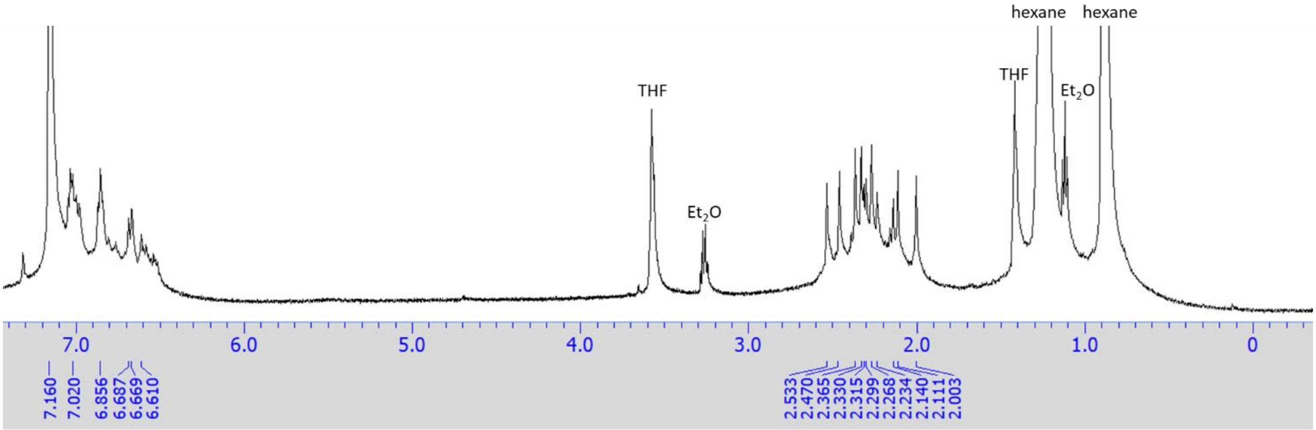

Figure S13. ^{1}H NMR spectrum after reaction of compound **1** with 5 equivalents of selenium (C_6D_6, 500 MHz).

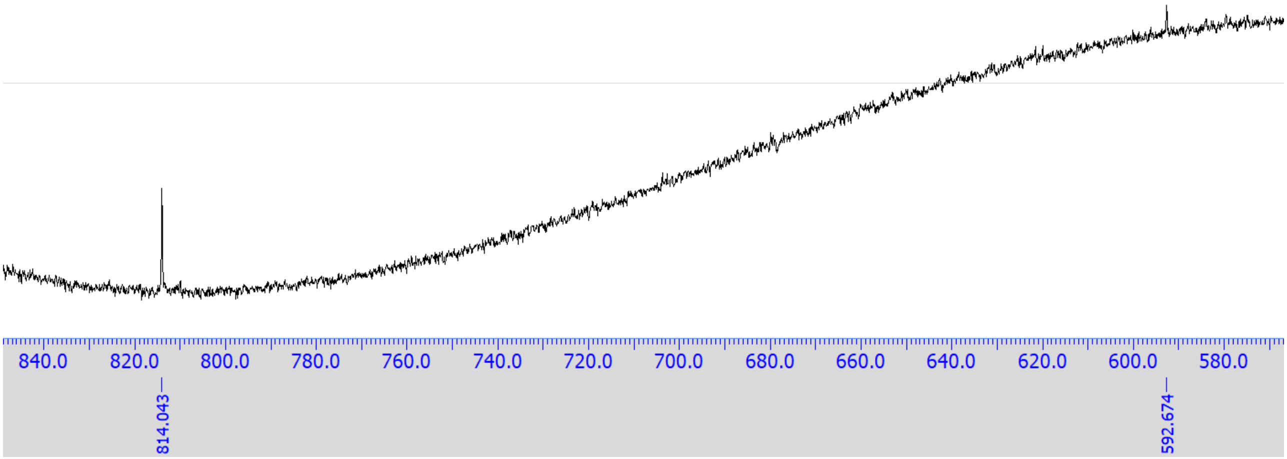

Figure S14. ^{77}Se NMR spectrum after reaction of compound **1** with 5 equivalents of selenium (C_6D_6, 95.4 MHz).

III. IR Spectra

Compound **2**

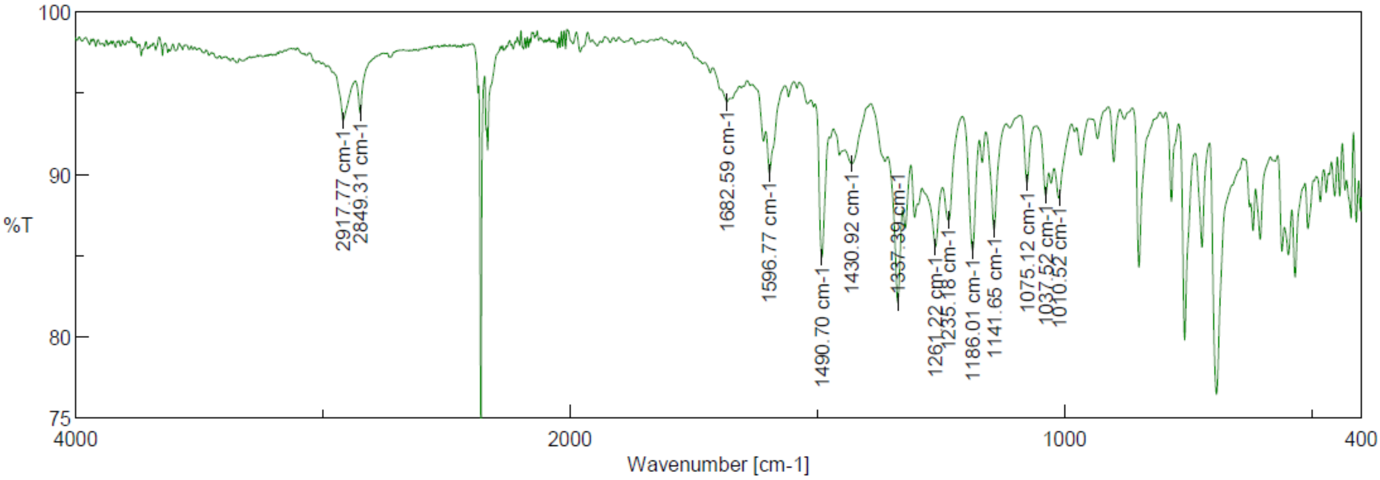

Figure S15. IR (ATR) spectrum for compound **2**.

Compound **3**$_S$

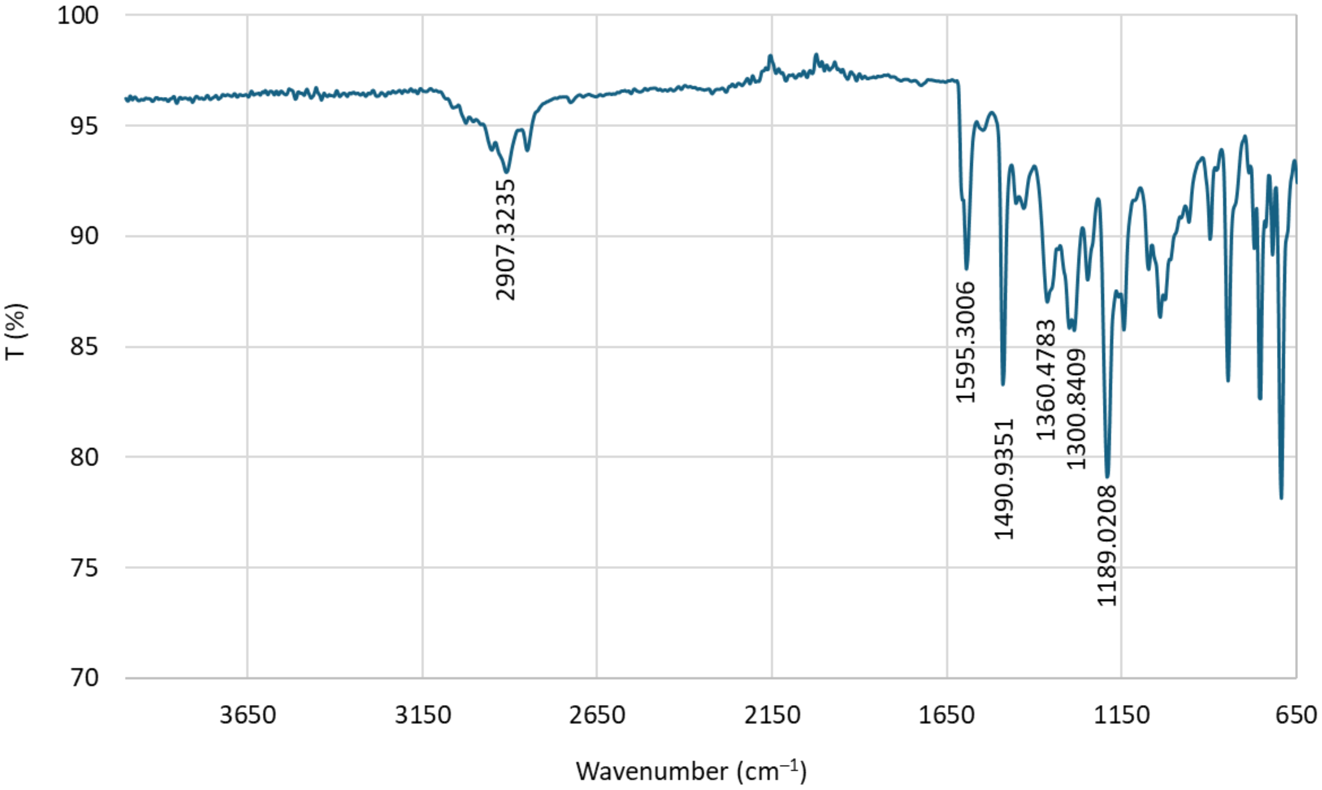

Figure S16. IR (ATR) spectrum for compound **3**$_S$.

IV. Detail for the X-ray Crystallographic Analyses

IV-I. Instrumentation

X-ray crystallographic analyses of single crystals were performed on a Rigaku VariMax with hybrid photon counting detector. A single crystal was mounted with mineral oil on a loop-type mount and transferred to the goniometer. The radiation was performed with graphitemonochromated Mo Kα (λ = 0.71073 Å) at 50 kV and 24 mA. The structures were solved by the direct method with (SHELXT 2018) and refined by full-matrix least-squares techniques against F^2 (SHELXL 2018). The intensities were corrected for Lorentz and polarization effects. The nonhydrogen atoms were refined anisotropically.

IV-II. Crystallographic Data

Table S1. Data for compounds **2** and **3_{Se}**.

		2	**3_{Se}**
CCDC number		2357519	2357520
Empirical formula		$C_{31}H_{32}B_2N_2$	$C_{62}H_{64}B_4N_4Se$
Formula weight		454.20	987.37
Temperature (K)		93(2)	93(2)
Wavelength (Å)		0.71073	0.71073
Crystal system		Orthorhombic	Orthorhombic
Space group		*Pbcn*	$P2_12_12$
Unit cell dimensions	a (Å)	15.9465(4)	23.3386(7)
	b (Å)	14.8115(4)	22.7872(6)
	c (Å)	22.4995(7)	12.1836(4)
	α (°)	90	90
	β (°)	90	90
	γ (°)	90	90
Volume (Å^3)		5314.2(2)	6479.5(3)
Z		8	4
Density (calculated) (g/m^3)		1.135	1.012
Absorption coefficient (mm^{-1})		0.065	0.615
F(000)		1936	2072
Theta (max)		29.8400	29.6060
Index ranges		–21≦h≦21	–31≦h≦31
		–19≦k≦20	–31≦k≦30
		–30≦l≦25	–16≦l≦16
Reflections collected		42031	60274
Independent reflections [R(int)]		6786 [R(int) = 0.0300]	15647 [R(int) = 0.0328]
Data Completeness (%)		0.999	0.996
Refinement method		Multi-scan	Multi-scan
Data / restrains / parameters		6786/0/322	15647/0/652
Goodness-of-fit on F^2		1.045	1.048

Final R indices [I>2σ(I)]	R_1 = 0.0464, wR_2 = 0.1264	R_1 = 0.0357, wR_2 = 0.0948
R indices (all data)	R_1 = 0.0534, wR_2 = 0.1326	R_1 = 0.0409, wR_2 = 0.0972
Largest diff. peak and hole (e.Å^{-3})	0.465/–0.285	0.438/–0.268

Table S2. Data for compound **3**$_\mathrm{S}$ and a mixture of compounds **4** and **5** in 15 : 85 ratio.

		3$_\mathrm{S}$	**4** and **5** (15 : 85)
CCDC number		2381240	2381489
Empirical formula		$C_{62}H_{64}B_4N_4S$, C_3H_7	$C_{62}H_{64}B_4N_4Se_{4.85}$
Formula weight		983.55	1291.36
Temperature (K)		93(2)	93(2)
Wavelength (Å)		0.71073	0.71073
Crystal system		Monoclinic	Orthorhombic
Space group		$P12_1/n1$	$Pbca$
Unit cell dimensions	a (Å)	15.6639(6)	14.4403(4)
	b (Å)	16.1414(7)	25.7841(9)
	c (Å)	23.3110(10)	32.0022(11)
	α (°)	90	90
	β (°)	93.896(4)	90
	γ (°)	90	90
Volume (Å^3)		5880.3(4)	11915.4(7)
Z		4	8
Density (calculated) (g/m^3)		1.111	1.440
Absorption coefficient (mm^{-1})		0.097	3.024
F(000)		2100	5191
Theta (max)		27.8170	28.0910
Index ranges		–20≦h≦20	–18≦h≦19
		–19≦k≦21	–32≦k≦35
		–26≦l≦31	–41≦l≦43
Reflections collected		64257	116527
Independent reflections [R(int)]		13621 [R(int) = 0.0683]	15390 [R(int) = 0.0803]
Data Completeness (%)		0.999	0.999
Refinement method		Multi-scan	Multi-scan
Data / restrains / parameters		13621/0/680	15390/4/716
Goodness-of-fit on F^2		1.018	1.071
Final R indices [I>2σ(I)]		R_1 = 0.0561, wR_2 = 0.1238	R_1 = 0.0575, wR_2 = 0.1209
R indices (all data)		R_1 = 0.1030, wR_2 = 0.1424	R_1 = 0.0941, wR_2 = 0.1327
Largest diff. peak and hole (e.Å^{-3})		0.673/–0.485	1.774/–0.523

V. Method and Discussion for Theoretical Calculation

V-I. General

DFT calculations were performed using the Gaussian 16 revision C.01 Program. For V-II to VII, geometry optimizations followed by frequency calculations were performed using M06-2X functional and 6-311G(d,p) basis set. For V-VIII, M06 functional and Lanl2DZ (for Se), 6-31G(d) (for others) basis set was employed. For natural bond orbital (NBO) analyses, NBO 6.0 was employed.

V-II. Effect of Boryl Substitution on C–C Double Bond

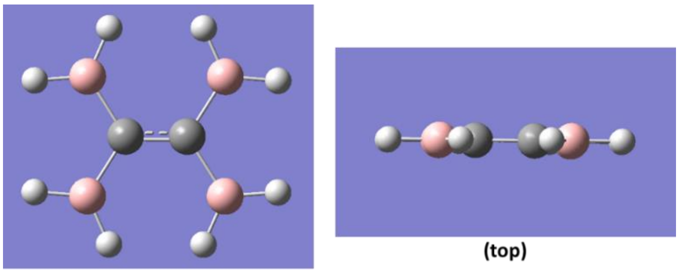
(front) (top)

Figure S17. Optimized structure of $(H_2B)_2C{=}C(BH_2)_2$.

- LUMO (–3.13 eV)

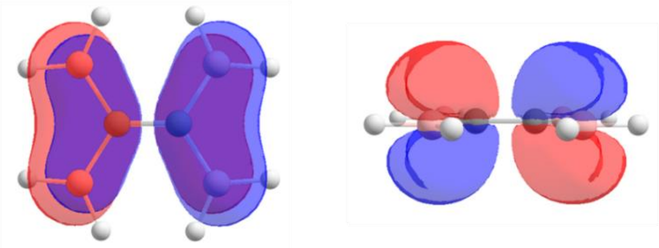
(front) (top)

- HOMO (–9.02 eV)

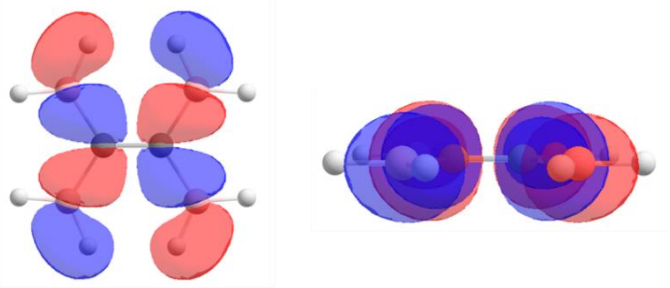
(front) (top)

- HOMO–2 (–10.3 eV)

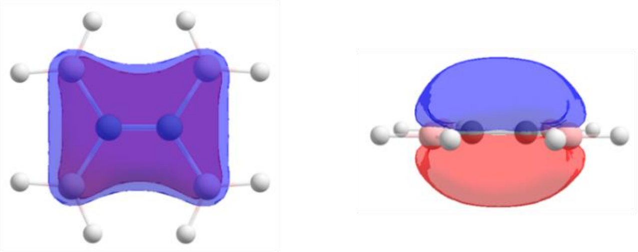
(front) (top)

Figure S18. Molecular orbitals of $(H_2B)_2C{=}C(BH_2)_2$.

Table S3. Selected parameters of ethylene and $(H_2B)_2C{=}C(BH_2)_2$.

	d(C=C) (Å)	E($\pi_{C=C}$) (eV)	E($\pi^*_{C=C}$) (eV)	Occupancy of $\pi_{C=C}$
$H_2C{=}CH_2$	1.32	–9.08	+1.35	2.00
$(H_2B)_2C{=}C(BH_2)_2$	1.38	–10.3	–3.13	1.74

As shown in Figure S17, $(H_2B)_2C{=}C(BH_2)_2$ showed a perfectly planar structure wherein all the four vacant p-orbitals on the boron atoms were aligned parallel to the π-orbital of the C=C moiety. Contribution of the boron atoms to the π-conjugation system was confirmed for both C=C π-bonding and antibonding orbitals, which were found at HOMO–2 and LUMO, respectively (Figure S18). Table S3 has summarized the selected parameters of the optimized structures of ethylene and $(H_2B)_2C{=}C(BH_2)_2$. C–C double bond length of $(H_2B)_2C{=}C(BH_2)_2$ was longer than ethylene (1.38 Å for $(H_2B)_2C{=}C(BH_2)_2$ and 1.32 Å for ethylene, respectively). $\pi^*_{C=C}$ of $(H_2B)_2C{=}C(BH_2)_2$ was quite lower-lying than that of ethylene owing to the contribution of p-orbitals on the boron atoms. NBO analysis clearly showed the withdrawal of π-electrons from C=C moiety by the boryl groups; electron occupancy of $\pi_{C=C}$ decreased from 2.00 for ethylene to 1.74 for $(H_2B)_2C{=}C(BH_2)_2$ by the introduction of boryl groups.

V-III. Optimized Structure of Compound 2

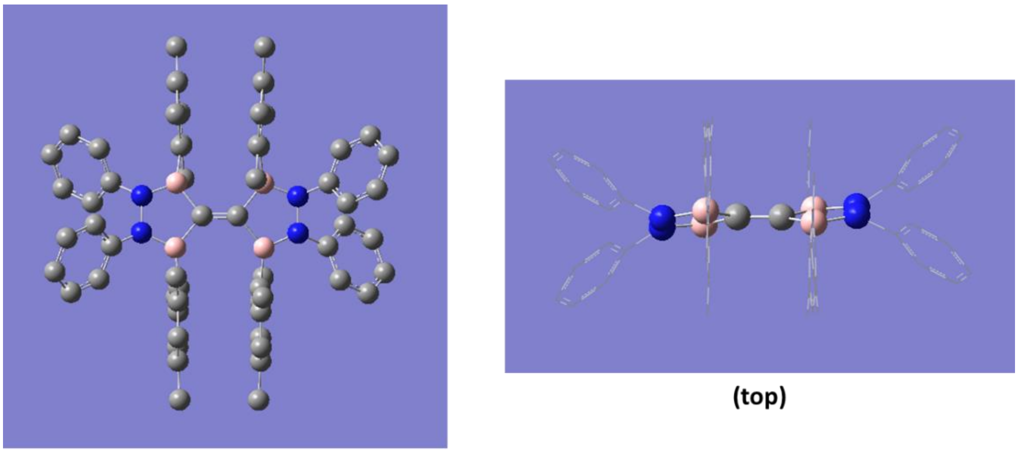

(front)

(top)

Figure S19. Optimized structure of compound **2**. Hydrogen atoms are omitted for clarity. In the top view, aromatic substituents on the boron and nitrogen atoms are shown in wireframe style for clarity.

Table S4. Comparison between optimized and X-ray structures of compound **2** on selected structural parameters.

	X-ray structure	**Optimized structure**
C=C (Å)	1.368(2)	1.360
C–B (Å)	1.5957(15), 1.6004(15)	1.595, 1.596
B–N (Å)	1.4174(15), 1.4206(15)	1.421, 1.422
B–C–B (°)	102.79(8)	102.99
B–C–C–B (°)	17.21, 26.96	15.35, 22.63

V-IV. S–T Gap of Compound 2

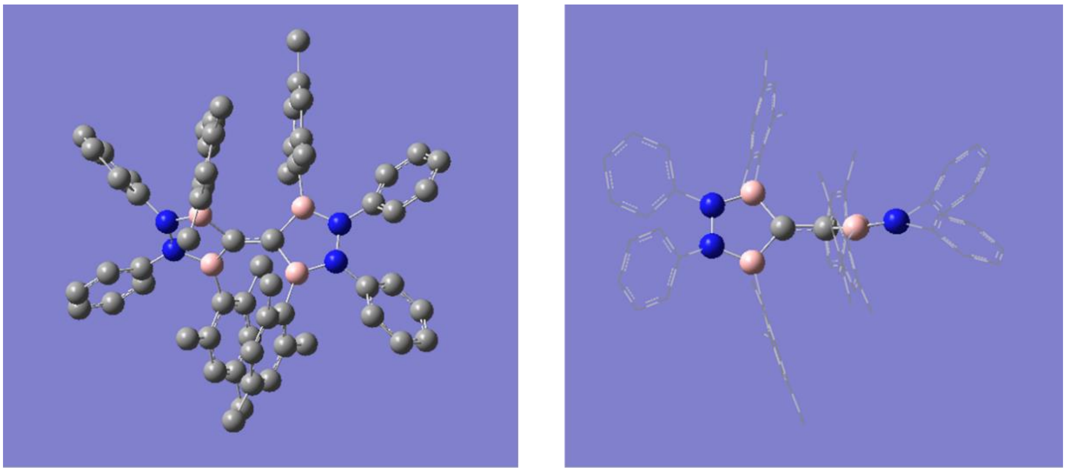

(front) (top)

Figure S20. Optimized structure of compound **2** in a triplet state. (C=C: 1.412 Å, B–C–C–B: 66.25°, 66.26 °)

Compound **2** takes a ground singlet state with an S–T gap of 27.8 kcal/mol. Compound **2** in a triplet state has a highly twisted geometry with a torsion angle of about 66°, and the central C–C double bond is elongated.

V-V. Dissociation Energy of Tetraborylethylene 2 into Two DBC Molecules

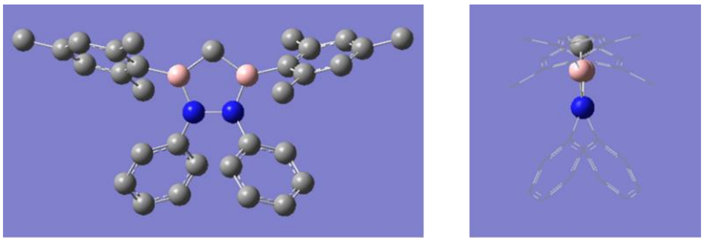

(front) (side)

Figure S21. Optimized structure of triplet DBC.

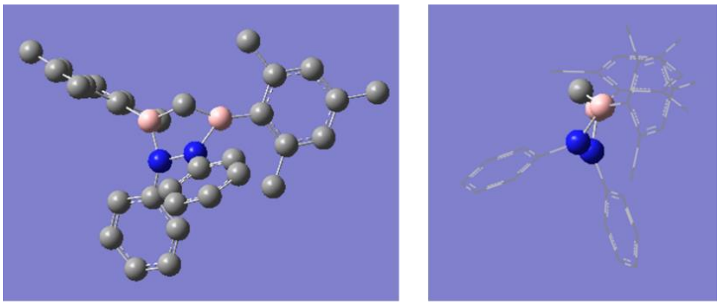

(front) (side)

Figure S22. Optimized structure of singlet DBC.

Table S5. Free energy of triplet TBE **2**, two molecules of triplet/singlet DBC relative to singlet TBE **2**.

TBE **2** (singlet)	TBE **2** (triplet)	Two DBC molecules (triplet)	Two DBC molecules (singlet)
0 kcal/mol	27.8 kcal/mol	137 kcal/mol	149 kcal/mol

V-VI. Effect of Bulky Substituents on the Boron Atoms

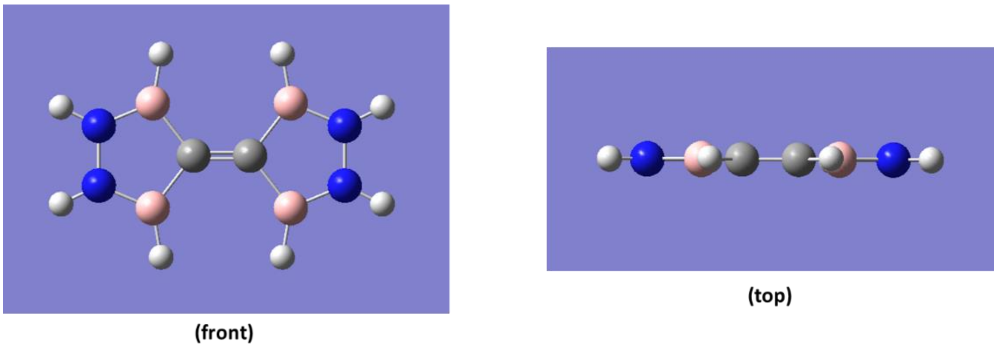
(front) (top)

Figure S23. Optimized structure of simplified tetraborylethylene **2'**.

Table S6. Comparison between optimized structures of **2** and **2'** on selected structural parameters.

	Compound 2 (Mes on B and Ph on N)	**Compound 2' (H on B and N)**
C=C (Å)	1.360	1.353
C–B (Å)	1.595, 1.596	1.582
B–C–C–B (°)	15.35, 22.63	0.00

Simplified structure **2'** showed a smaller torsion angle, which indicates that the steric repulsion between facing mesityl groups has a significant effect on the obtained X-ray structure of **2**.

V-VII. Molecular Orbitals of Compound 2 and Related Molecules

a) Ethylene

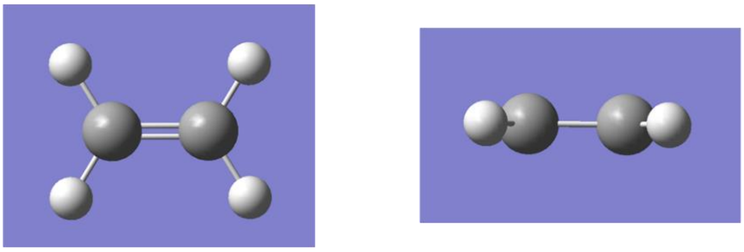

(front) **(top)**

b) Fulvalene

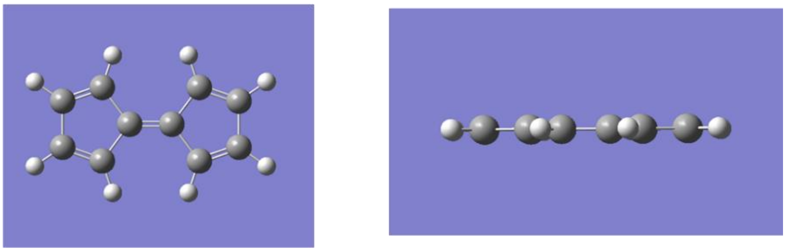

(front) **(top)**

c) Tetrathiafulvalene

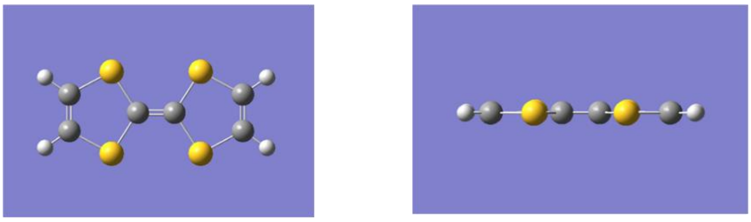

(front) **(top)**

d) Compound I

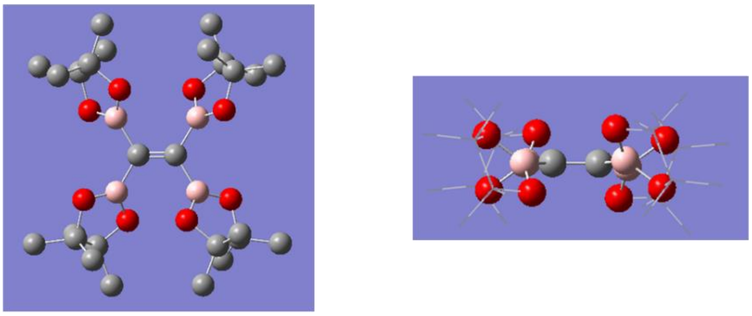

(front) **(top)**

Figure S24. Optimized structures of (a) ethylene, (b) fulvalene, (c) tetrathiafulvalene, and (d) compound **I** ($(pinB)_2C{=}C(Bpin)_2$). It should be noted that the optimized structure of compound **I**, wherein all Bpin groups are twisted, did not reproduce its X-ray structure.

- LUMO (+1.35 eV)

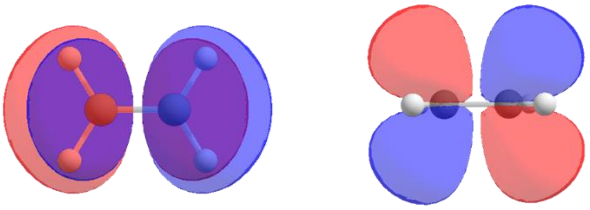

(front) (top)

- HOMO (–9.08 eV)

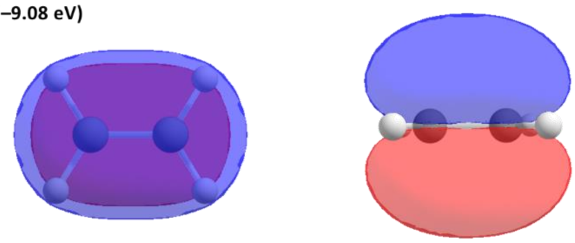

(front) (top)

Figure S25. Molecular orbitals of ethylene.

- LUMO (–2.09 eV)

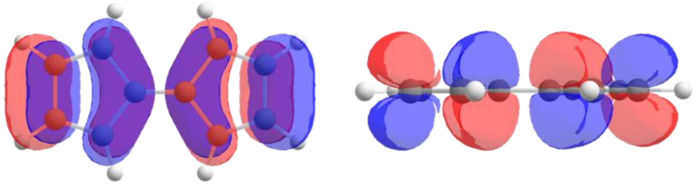

(front) (top)

- HOMO (–7.59 eV)

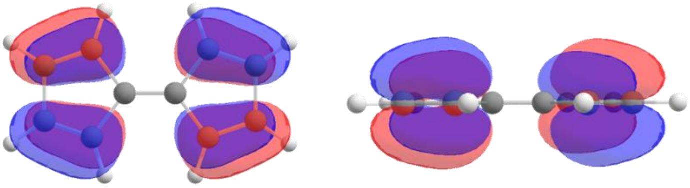

(front) (top)

- HOMO–2 (–8.14 eV)

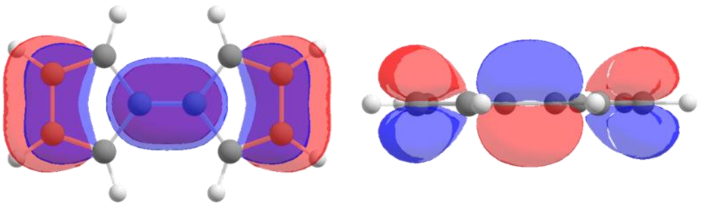

(front) (top)

Figure S26. Molecular orbitals of fulvalene.

- LUMO+3 (+1.05 eV)

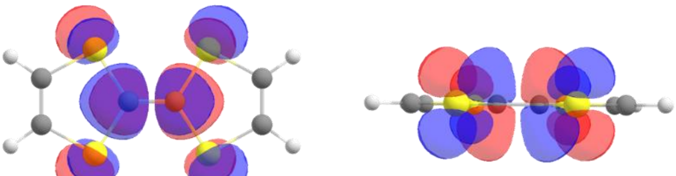

(front) **(top)**

- LUMO (0.00 eV)

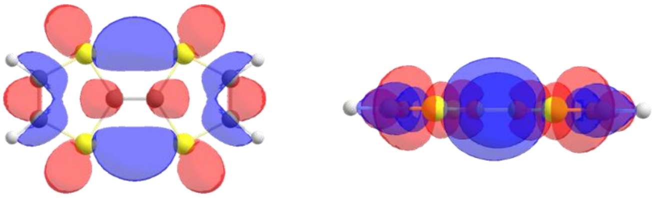

(front) **(top)**

- HOMO (–5.81 eV)

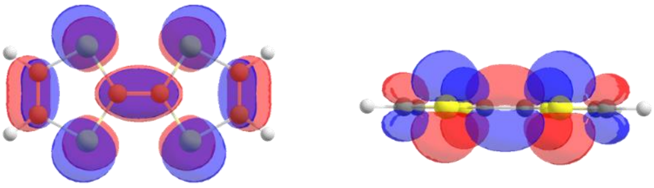

(front) **(top)**

Figure S27. Molecular orbitals of tetrathiafulvalene.

- LUMO (–0.17 eV)

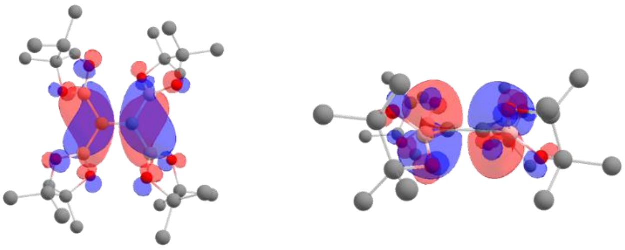

(front) **(top)**

- HOMO (–8.47 eV)

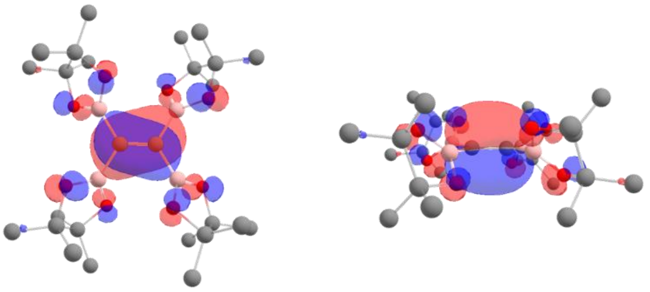

(front) **(top)**

Figure S28. Molecular orbitals of compound **I**.

- LUMO (–1.75 eV)

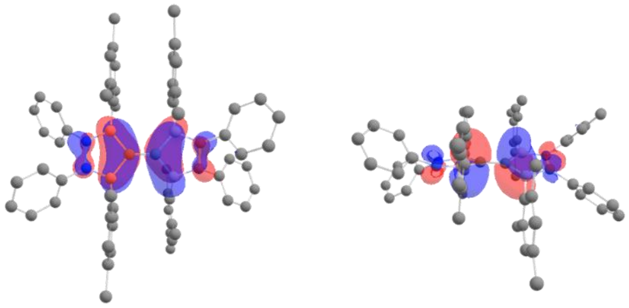

(front) (top)

- HOMO (–6.84 eV)

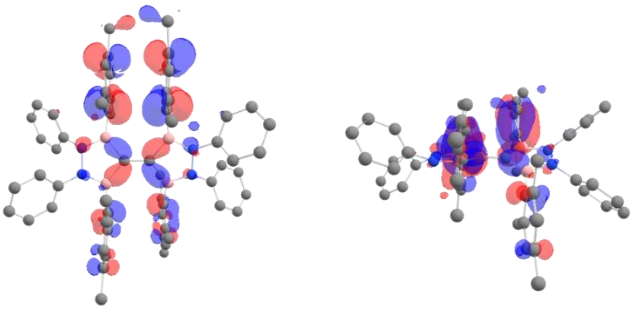

(front) (top)

- HOMO–17 (–9.23 eV)

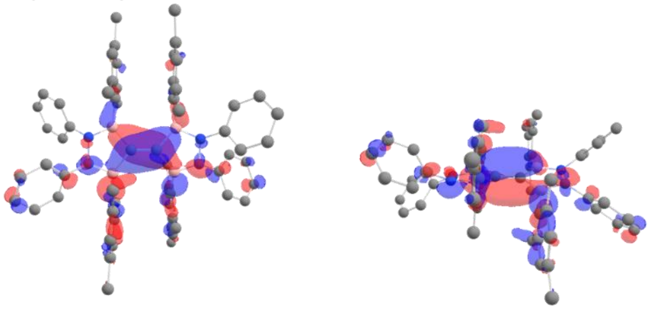

(front) (top)

Figure S29. Molecular orbitals of compound **2**.

V-VIII. Elimination of Chalcogen Atom from Bis(diborylmethylene)-λ^4-chalcogenane

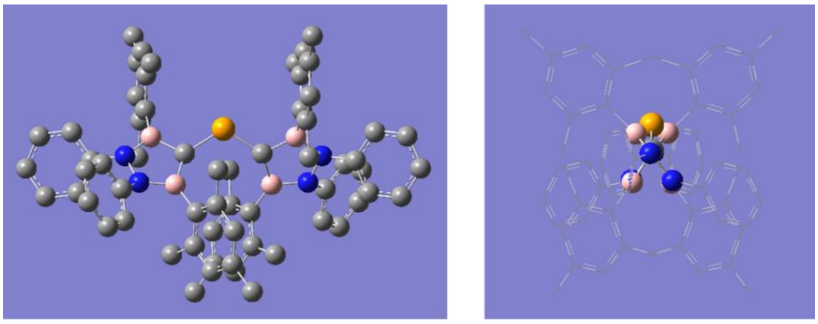
(front) (side)

Figure S30. Optimized structure of compound **3**$_{\mathbf{Se}}$. Hydrogen atoms are omitted for clarity. In the side view, aromatic substituents are shown in wireframe style for clarity.

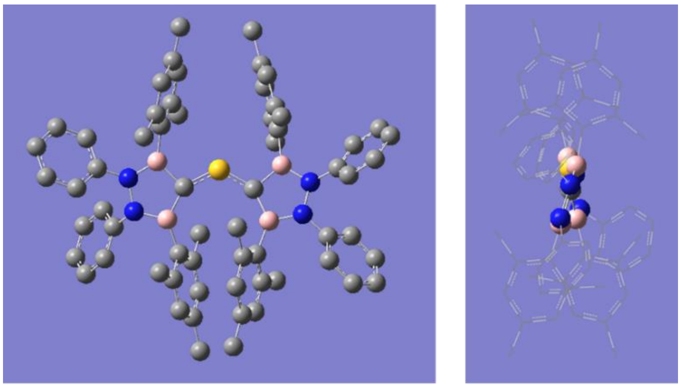
(front) (side)

Figure S31. Optimized structure of compound **3**$_{\mathbf{S}}$. Hydrogen atoms are omitted for clarity. In the side view, aromatic substituents are shown in wireframe style for clarity.

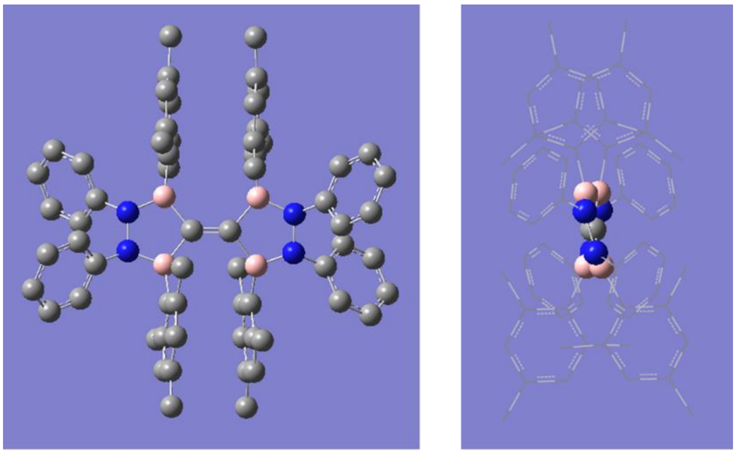
(front) (side)

Figure S32. Optimized structure of compound **2**. Hydrogen atoms are omitted for clarity. In the side view, aromatic substituents are shown in wireframe style for clarity.

Table S7. Energy comparison between before and after elimination of chalcogen atom from compound **3**$_{\mathbf{Ch}}$.

	(i) Compound **3**$_{\mathbf{Ch}}$ (a.u.)	(ii) TBE **2** + Ch atom (a.u.)	⊿E ((ii)–(i)) (kcal/mol)
Selenium	–2725.76886	–2725.793992	–15.8
Sulfur	–3114.827806	–3114.71042	73.7

VI. UV-Vis Measurement of Compound 2

VI-I. General

1.0 mg of compound **2** was dissolved in 10 mL of benzene, and the solution was put in a quartz cell with a screw cap (3.5 mL) in a glovebox. UV-Vis spectra were recorded on a SHIMADZU UV-3150 spectrophotometer. TD-DFT calculation of compound **2** was conducted using M06-2X/6-311G(d,p) level of theory on the optimized structure at the same level of theory.

VI-II. Absorption Spectrum

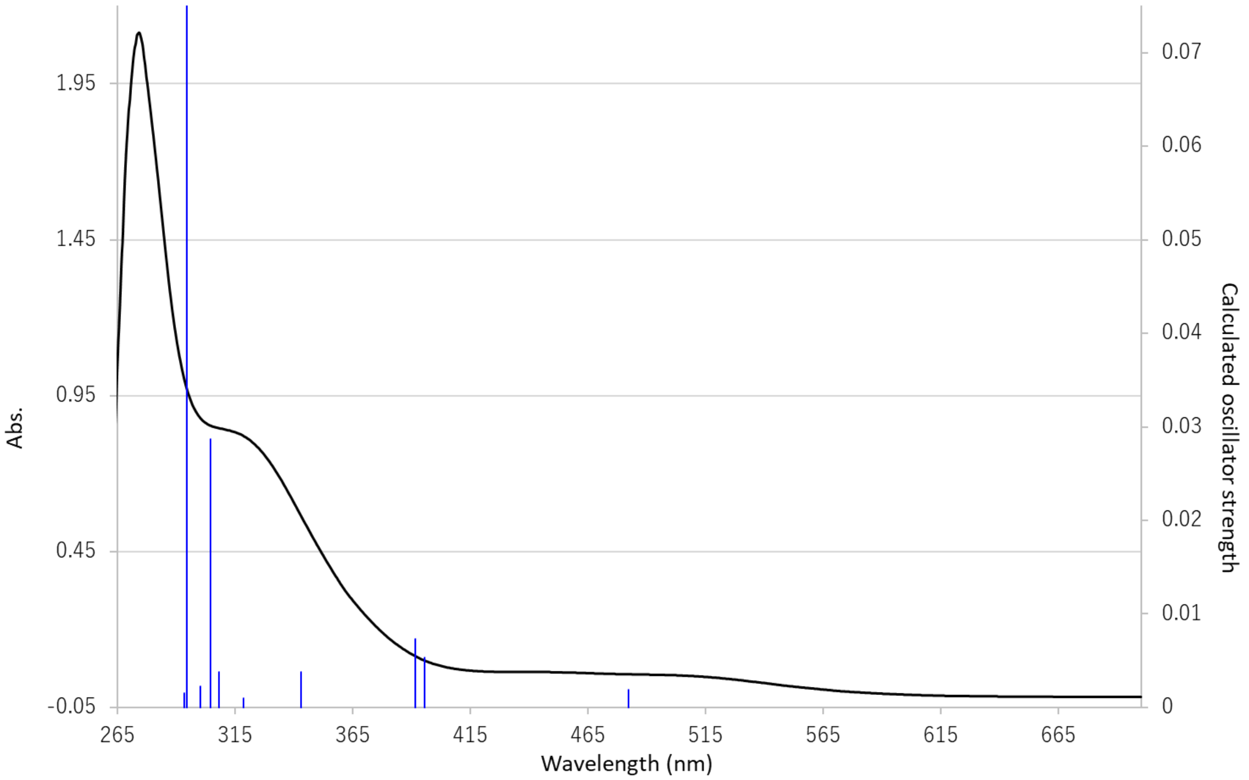

Figure S33. UV-Vis spectrum of compound **2** (black, 1×10^{-5} M in C_6H_6). Theoretically obtained absorptions are overlapped with the experimentally obtained spectrum (blue).

VII. CV and DPV Measurements

VII-I. General

Cyclic voltammetry (CV) experiments were carried out in THF solution of **2** (1.0 mM) containing ^{n}Bu$_4$NPF$_6$ (0.10 M) as a supporting electrolyte with scan rates of 100 mV/s or 20 mV/s using Ag/Ag$^+$ as the reference electrode, Pt as the working electrode, and Pt wire as the counter electrode. The potential was calibrated against Fc/Fc$^+$.

VII-II. CV, DPV Charts

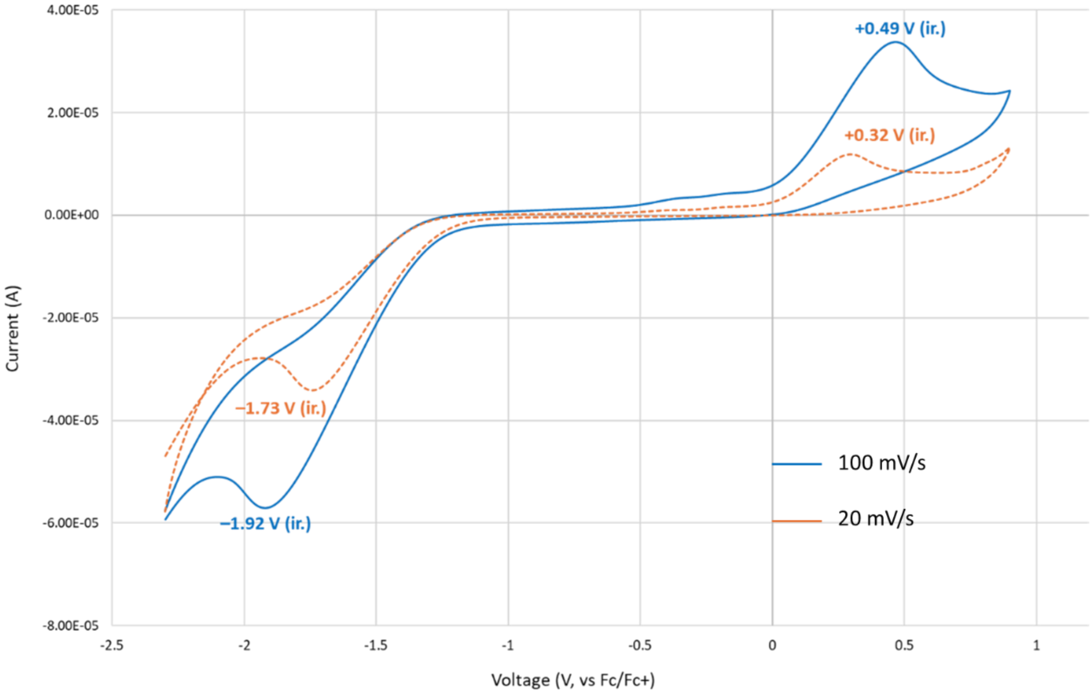

Figure S34. CV chart of compound **2**.

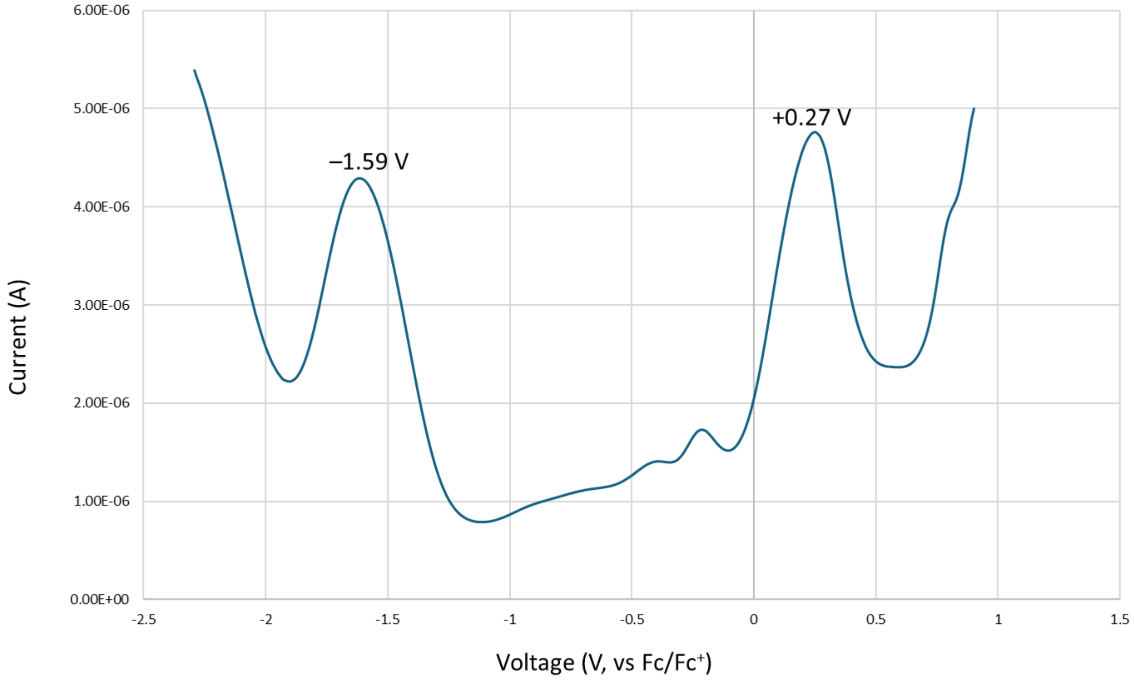

Figure S35. DPV chart of compound **2**.

VIII. Luminescence Quenching Experiment

VIII-I. General

i) Solution preparation

fac-Ir(ppy)$_3$: 5.0 mg of *fac*-Ir(ppy)$_3$ was dissolved in 10 mL of THF (0.38 mM).

TBE **2**: 15.1 mg of TBE **2** was dissolved in 5 mL of THF (3.3 mM).

ii) Sample preparation

	fac-Ir(ppy)$_3$	TBE **2**	Total
Sample 1	1.0 mL (0.11 mM)	0 mL (0 mM)	3.5 mL
Sample 2	1.0 mL (0.11 mM)	25 μL (0.024 mM)	3.5 mL
Sample 3	1.0 mL (0.11 mM)	50 μL (0.049 mM)	3.5 mL
Sample 4	1.0 mL (0.11 mM)	100 μL (0.098 mM)	3.5 mL

VIII-II. Emission Spectra (excited at 450 nm) and Stern-Volmer Plot

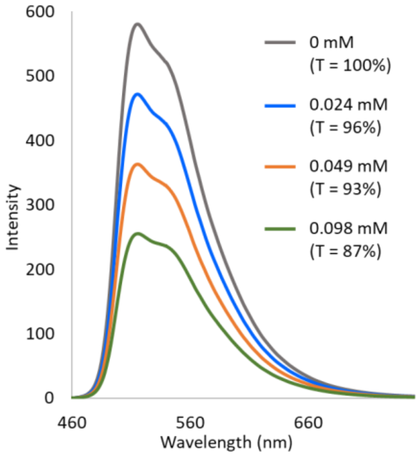

Figure S36. Emission spectra of *fac*-Ir(ppy)$_3$ in THF under coexistence of compound **2**. T means the transmittance of the excitation light (450 nm) by TBE **2**.

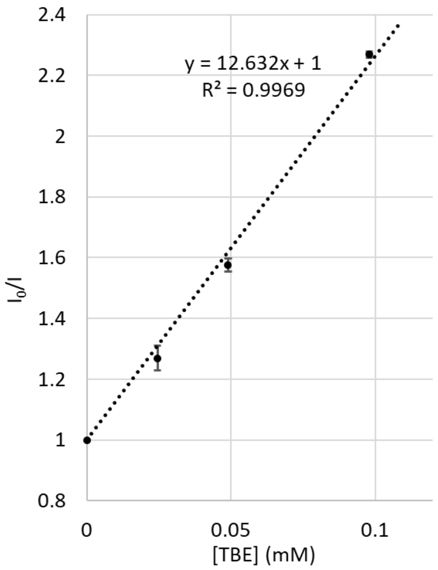

Figure S37. Stern-Volmer plot for compound **2**. Intensity at 510 nm was employed to make the plot.

IX. References

[1] Pangborn, A. B., Giardello, M. A., Grubbs, R. H., Rosen, R. K. & Timmers, F. J. Safe and Convenient Procedure for Solvent Purification. *Organometallics* **1996**, *15*, 1518–1520.

[2] Shibutani, Y., Kusumoto, S., Nozaki, K. Synthesis, Characterization and Trapping of a Cyclic Diborylcarbene, an Electrophilic Carbene. *J. Am. Chem. Soc.* **2023**, *145*, 16186–16192.